

Limit speeds and stresses in power law functionally graded rotating disks

Royal Madan^{*1}, Kashinath Saha² and Shubhankar Bhowmick^{1a}

¹ Department of Mechanical Engineering, National Institute of Technology Raipur (C.G)-492010, India

² Department of Mechanical Engineering, Jadavpur University, Kolkata 700032, India

(Received January 1, 2020, Revised April 18, 2020, Accepted May 13, 2020)

Abstract. Limit elastic speed analysis of Al/SiC-based functionally graded annular disk of uniform thickness has been carried out for two cases, namely: metal-rich and ceramic rich. In the present study, the unknown field variable for radial displacement is solved using variational method wherein the solution was obtained by Galerkin's error minimization principle. One of the objectives was to identify the variation of induced stress in a functionally graded disk of uniform thickness at limit elastic speed using modified rule of mixture by comparing the induced von-Mises stress with the yield stress along the disk radius, thereby locating the yield initiation. Furthermore, limit elastic speed has been reported for a combination of varying grading index (n) and aspect ratios (a/b). Results indicate, limit elastic speed increases with an increase in grading indices. In case of an increase in aspect ratio, limit elastic speed increases up to a critical value beyond which it recedes. Also, the objective was to look at the variation of yield stress corresponding to volume fraction variation within the disk which later helps in material tailoring. The study reveals the qualitative variation of yield stress for FG disk with volume fraction, resulting in the possibility of material tailoring from the processing standpoint, in practice.

Keywords: yield stress calculation; modified rule of mixture (MROM); limit analysis; variational method; FG disk

1. Introduction

A functionally graded material helps to attain functional-based requirements in a component; the objective is to manufacture application based material in which metal-metal, metal-ceramic or ceramic-ceramic are combined either in stepwise or continuously graded manner. In Mortensen and Suresh (1995), two principal processes of functionally graded manufacturing; constructive and transport based processes; are defined of which constructive processes allow designers to program and produce gradients without any restrictions. The processing principles focus on making the best use of available material and to avoid stress and strain concentrations at the interface during loading. The component produced thus possess properties like low weight, high-temperature resistance, corrosion resistance, and high toughness to name a few which have wide applications in area like aerospace (rocket nozzle and engine components), nuclear energy (nuclear reactor), electronics

*Corresponding author, Scholar, E-mail: rmadan.phd2017.mech@nitrr.ac.in

^a Ph.D., E-mail: sbhowmick.mech@nitrr.ac.in

(semiconductor), power plants (turbine blade), biomaterial (implants and artificial skin), commodities (sports bike), defense (bullet-proof vests) chemical plant (heat exchanger) in cutting tools and data storage devices (Miyamoto *et al.* 1999). In Mahamood and Akinlabi (2017), fabrication of FGM is classified into two broad groups namely thin and bulk; the former is produced using vapour deposition techniques, high-temperature synthesis, plasma spraying, and other similar techniques, while the latter is produced using centrifugal casting, powder metallurgy (P/M) processes, etc. Centrifugal casting and powder metallurgy have proven effective in the fabrication of FGM. Though under centrifugal casting method continuous gradation is achieved but still, P/M is an attractive process because it provides excellent control over microstructure, including size, morphology and volume fraction of matrix and reinforcement. The fabricated P/M parts have many structural and thermal applications (Madan and Bhowmick 2020) and with growing interests of FGM's in the area of MEMS/NEMS which has applications in communications, machinery, information technology, and biotechnology technologies, used in the form of beams, plates, and membranes (Ebrahimi *et al.* 2015); to design such structures, study of their vibration behavior under different mechanical and thermal loading is essential. In Ebrahimi *et al.* (2016), Ebrahimi and Salari (2016), authors studied the effects of temperature change, gradient indexes, small scale parameter, mode number and boundary conditions on the natural frequencies of the temperature-dependent FG nanobeams for P-FGM variation, under different thermal loading. A differential transformation method (DTM) is proposed in Ebrahimi and Salari (2015) and performed a thermo-mechanical vibration analysis of FG nano-beams with various boundary conditions. Using DTM, an exact solution for the differential equation is possible in less time with good precision. In Saif *et al.* (2019), identified the failure reasons for turbine blades in which the primary reason analyzed was a material defect and secondary, creep at the tip.

Power-law, functional grading of disk subjected to centrifugal forces and thermal loading was studied by Kordkheili and Naghdabadi (2007) wherein the stresses and displacement components in the disk were reported. Later Bayat *et al.* (2008), for similar material grading, studied the effects of different disk profiles such as concave, convex and linear variation, and found converging thickness to be better than constant thickness disk and divergent disk profiles. Material tailoring, to maintain constant tangential stress was reported by Nie and Batra (2010) wherein an arbitrary radial variation of shear modulus was obtained. In Nejad *et al.* (2014), elasto-plastic analysis of FGM disk for density variation was studied based on a power-law variation of elastic modulus, density and reported yield limit and plastic flow zones for different inhomogeneity constants using Tresca yield criteria. A similar variation in mechanical properties was considered by Çallioğlu *et al.* (2015) for different angular velocity, uses von Mises yield condition and observed that the region of yielding propagates towards the periphery of the disk for non-work hardening case and increasing angular speed. Variational formulation method has been employed by Bhowmick *et al.* (2008) for the attached mass in solid disk considering different disk profiles and loading parameters. The method was extended in Bhowmick *et al.* (2009) to analyze the yield propagation in an annular disk and then for solid disk in Bhowmick *et al.* (2010) under elasto-plastic regime by assuming linear hardening behavior. The similar variational method was extended by Nayak and Saha (2016) to study limit stresses under thermo-mechanical load for both solid and annular disk by changing disk profiles and varying temperatures. There are studies where an optimal composition of composites has been identified using optimization techniques like TOPSIS (Jha *et al.* 2018). For solid disk elasto-plastic stress field and critical angular velocity were calculated by Jahromi *et al.* (2012) using a modified rule of mixture, the solution was obtained using extended variable material property (VMP).

In Mahdavi *et al.* (2016), uses power-law mechanical property variation as given by Kordkheili and Naghdabadi (2007) for convergent, divergent and uniform thickness disk considering metal-rich (6061-T6 Al alloy) at inner radius and ceramic-rich (ZrO_2) at the outer radius. Solutions obtained using variable material property reveals yielding location was at the root for uniform thickness disk and can be anywhere for variable thickness disk. In Zheng *et al.* (2016), the authors arrived at the similar property variation as given by Kordkheili and Naghdabadi (2007) for power-law variation of volume fraction, studied the effect of acceleration on FG disks bearing same mass. Smaller stresses were obtained by designing smaller thicknesses at the periphery in case of the ceramic rich zone at the inner radius. During fabrication of FGM porosity may come due to technical reasons, hence, to estimate effectively the material properties of FGM using a rule of mixture requires a calculation of porosity effects as well. In Hamed *et al.* (2019) studied the porosity effects on a static deflection for four different models of porosities incorporated with the ROM model. An evenly distributed porosity model used by Abderezak *et al.* (2018) to investigate interfacial stresses in damaged reinforced concrete beams bonded with a functionally graded material plate under uniform loading. In Ebrahimi *et al.* (2017), Ebrahimi and Jafari (2016), a power law is modified to approximate even and uneven porosity distributions in FG nano-beams. For different thermal loadings, namely, uniform, linear, nonlinear, and sinusoidal temperature rises, vibration analysis is performed for temperature-dependent material properties and the problem was solved using Navier type solution method. In Nakamura *et al.* (2000), developed relations for effective yield stress estimation and modified elastic modulus, the relation consists of single unknown parameter stress to strain transfer ratio (q) which is a slope between two materials were discussed. In another study, Bhattacharyya *et al.* (2007) performed an experimental analysis to determine ratio (q) for Al/SiC material. Reported results shows the estimation of Young's modulus with experimental and rule of mixture whereas differs very largely.

Rotating disks are irreplaceable components in machineries and are utilized widely from power transmission assemblies to energy storage devices (e.g., flywheel, gears, clutches, disk brake, etc.). As these are mainly subject to centrifugal loading and are designed to work with in elastic limit, any improvement in limit elastic capacity of the rotating disk straightaway increases its range of performance thereby improving its applicability. Functional tailoring of material properties has been reported to improve the limit elastic capacity of mechanical structures. In cases of rotating disks, such studies, though scarce, could help in providing an insight to metallurgists and design engineers about the anticipated variation in material grading suitable for particular applications. The typical problems of material, geometry or solution non-linearity makes the advent of approximation techniques a natural selection as compared to classical closed form methods. Amongst approximation methods, in terms of mathematical formulation using Variational method, it is a readily established weighted residual technique based on Galerkin's error minimization principle that has an advantage of being an economical solver as compared to finite element method due to its implementation over the entire domain with suitable combination of quadrature points and coordinate functions (resulting from convergence tests) (Bhowmick *et al.* 2008) instead of discretizing the domain into large number of elements and nodes and re-meshing the finite element space every time any changes in parameters are introduced into the study. There are various means by which material variations of FG rotating disk can be carried out such as, L-FGM, E-FGM (Madan *et al.* 2019b), S-FGM (Madan *et al.* 2019a) and others. Apart from these, there are material models that are used to estimate the material properties such as rule of mixture, modified rule of mixture, Mori-Tanaka, Halpin-Tsai (Madan *et al.* 2019c, Madan *et al.* 2020). The modified rule of mixture which is used in the present study estimates effectively the Young's modulus of particulate

reinforced composites in comparison to rule of mixture, it also gives an effective estimation of yield stress variation for FGM which is vital in case of limit studies (Madan *et al.* 2018). It is interesting to note that no study on limit elastic analysis which defines disk performance has been carried out by using MROM for P-FGM. Results are reported for stress distribution (radial, tangential and von Mises) along with yield stress variation in a disk at limit elastic angular speeds. Even though the stresses are higher at the root of the disk the yielding locations in uniform thickness disk for power-law grading are not always at the root but varies with grading indices (n) and aspect ratios (a/b). Shifting of yielding location other than root increases the limit elastic speed. And the identification of yielding locations unlocks a scope for further improvement in disk performance by going for different material tailoring or by additional reinforcement of different material at yielding locations.

2. Material grading

2.1 Volume fraction

A lot of literature has been reported in which material property is assumed directly such as; power law, exponential law or any other forms. In current work, material property variation is defined based on volume fraction variation, non-linear power-law variation was considered after substituting grading index (n) in Eq. (1) (Zheng *et al.* 2016). The material at the root of the disk is metal (aluminium) and at the tip of the disk is ceramic (silicon carbide). Two different cases of grading were taken: ceramic rich (ceramic composition is major) and metal-rich (metal composition is major), on substituting $n = 2, 3$, and 4 in Eq. (1) gives metal-rich and ceramic rich for $n = 1/2, 1/3$ and $1/4$.

$$V_c = \left(\frac{r - a}{b - a} \right)^n ; \quad V_m + V_c = 1 \quad (1)$$

Fig. 1 represents volume fraction variation of ceramic and metal to the normalized radius given by Eq. (1) for aspect ratio ($a/b = 0.1$). Similarly, composition variation for five different aspect ratios from 0.1 to 0.5 can be obtained by incrementing every time by 0.1 from the initial.

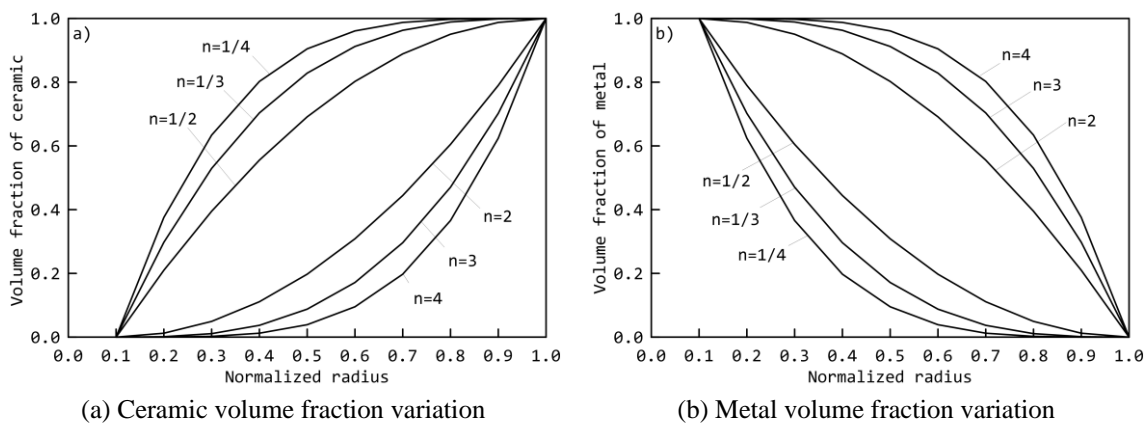


Fig. 1 Plot of volume fraction (non-linear) along disk radius for grading indices

2.2 Mass density

For density calculation, rule of mixture was used as given by Eq. (2), where the values of volume fraction are substituted for non-linear volume fraction as shown in Fig. 1. For pure aluminium and ceramic, the densities are taken as 2643 and 2130 Kg/m³ respectively.

$$\rho_f = \rho_m V_m + \rho_c V_c \quad (2)$$

2.3 Young's modulus of elasticity

Using modified rule of mixture (MROM), the effective modulus of elasticity was calculated using Eq. (3) (Nakamura *et al.* 2000), which has a parameter (q) associated with it. In composites, when a load is applied along fibre direction strain in each phase will be same ($\varepsilon_c = \varepsilon_m$) and stress in the component will be added up which is a Voigt model. Under transverse load, the stresses would be same ($\sigma_c = \sigma_m$) the resulting model is known as Reuss model. The overall Young's modulus from both the models are not sufficient to estimate the mechanical properties of particulate composites, hence, they are combined to obtain MROM.

$$E_f = \frac{V_c E_c + V_m E_m R}{V_c + V_m R} \quad (3)$$

$$\text{where } R = \frac{\bar{q}}{\bar{q} + \frac{E_m}{E_c}} \text{ and } \bar{q} = \frac{q}{E_c}$$

The modified Young's modulus given by Eq. (3) is a function of volume fraction of constituents as well as a parameter q . In Bhattacharyya *et al.* (2007), performed experiments taking different compositions of Al/SiC functionally graded material for three different mixings i.e., for 90/10, 80/20 and 70/30 and found that the variation in q for a change in mixing is negligible, hence, q can be assumed to be 91.6 GPa. Earlier in (Nakamura *et al.* 2000) the value of the ratio (q) was not known but after Bhattacharyya *et al.* (2007) performed experiments on Al/SiC material; knowing q , modified rule of mixture and yield stress calculation can be carried out for any mixing ratios.

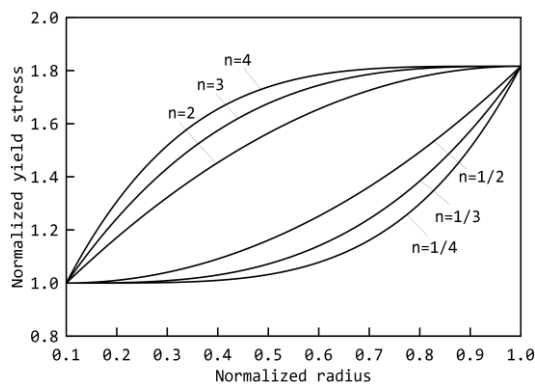


Fig. 2 Normalized yield stress with radius for $a/b = 0.1$

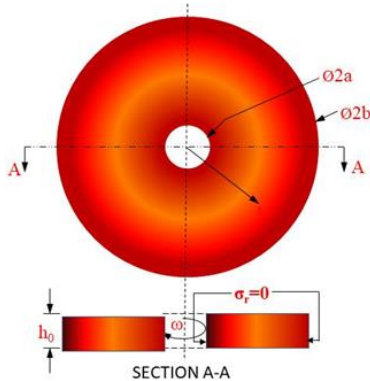


Fig. 3 Uniform thickness FG rotating disk

2.4 Yield stress distribution

Yield stress distribution was quantified using Eq. (4) given by Nakamura *et al.* (2000), and is shown in Fig. 2, the variation of yield stress is shown for different grading index, n , at constant aspect ratio ($a/b = 0.1$). Similarly, the variation of yield stress for different aspect ratios can also be calculated.

$$\sigma_y = \sigma_{ym} \left(V_m + \frac{E_c V_c}{E_m R} \right) \quad (4)$$

3. Mathematical formulation

A constant thickness disk of inner and outer radius a and b is considered as shown in Fig. 3. The disk rotates at an angular speed, ω . Assuming plane stress condition and employing variational principle by calculating the strain energy and external work done due to the above loading is given by Eqs. (5) and (6) respectively.

$$U = \frac{1}{2} \int_V (\sigma \varepsilon) dV = \frac{1}{2} \int_V (\sigma_\theta \varepsilon_\theta + \sigma_r \varepsilon_r) dV \quad (5)$$

$$V = - \int u \omega^2 r dm \quad (6)$$

Employing principle of minimum potential energy

$$\partial(U + V) = 0 \quad (7)$$

From stress-strain and strain-displacements relations, Eq. (7) takes the following form.

$$\delta \left[\frac{\pi}{1 - \mu^2} \int_a^b \left\{ E(r) \frac{u^2}{r} + E(r) 2\mu u \frac{du}{dr} + E(r) r \left(\frac{du}{dr} \right)^2 \right\} hdr - 2\pi \omega^2 \int_a^b \rho(r) r^2 u hdr \right] = 0 \quad (8)$$

Substituting normalized coordinate, as $\xi = (r-a)/(b-a)$, in Eq. (8) and taking $\bar{r} = b-a$, the following is obtained

$$\delta \left[\frac{\pi}{1-\mu^2} \int_a^b \left\{ E(r) \frac{u^2}{\xi} + E(r) 2\mu u \frac{du}{d\xi} + E(r) \xi \left(\frac{du}{d\xi} \right)^2 \right\} h d\xi - 2\pi\omega^2 b^3 \int_a^b \rho(r) \xi^2 u h d\xi \right] = 0 \quad (9)$$

The unknown displacement is approximated using a series of polynomial function as follows

$$u(\xi) = \sum c_i \varphi_i, \quad i = 1, 2, 3, \dots, n_f \quad (10)$$

In Eq. (10), φ_i are the set of orthogonal polynomials, of which the first function of the series is approximated as start function and the following higher-order orthogonal functions are calculated using the Gram–Schmidt scheme. The free-free boundary condition is employed as shown in Fig. 3.

$$\varphi_o(r) = \frac{\omega^2 r (3 + \mu)}{8} \left[\frac{\rho(r)}{E(r)} \left\{ (b^2 + a^2)(1 - \mu) - \frac{1 + 3\mu}{3 + \mu} r^2 + \frac{a^2 b^2}{r^2} (1 + \mu) \right\} \right] \quad (11)$$

Substituting Eq. (11) in Eq. (10), the algebraic integral form, thus becomes

$$\delta \left[\frac{\pi}{1-\mu^2} \int_0^1 \left\{ E(\xi) \left(\frac{(\sum c_i \varphi_i)^2}{\bar{r}\xi + a} + \frac{2\mu}{\bar{r}} \left[\sum c_i \varphi_i \frac{d(\sum c_i \varphi_i)}{d\xi} \right] + \frac{\bar{r}\xi + a}{r^2} \left(\frac{d(\sum c_i \varphi_i)}{d\xi} \right)^2 \right) \right\} \square d\xi \right. \\ \left. - 2\pi\omega^2 \int_0^1 \rho(\xi) \left\{ (\bar{r}\xi + a)^2 \sum c_i \varphi_i \right\} \square d\xi \right] = 0 \quad (12)$$

In Eq. (12), the variational operator (δ) is replaced by $\frac{\delta}{\delta c_j}$, $j = 1, 2, 3, 4, \dots, n_f$. Using Galerkin's error minimization principle; the algebraic equation obtained is as follows

$$\frac{\bar{r}}{1-\mu^2} \sum_{i=1}^n \sum_{j=1}^n c_i \int_0^1 E(\xi) \left\{ \frac{\varphi_i \varphi_j}{\bar{r}\xi + a} + \left(\frac{\mu}{\bar{r}} \left(\varphi_i' \varphi_j' \right) + \left(\frac{\bar{r}\xi + a}{\bar{r}^2} \right) (\varphi_i' \varphi_j') \right) \right\} h d\xi \\ = \omega^2 b^3 \sum_{i=1}^n \int_0^1 \rho(\xi) \{ (\bar{r}\xi + a)^2 \varphi_i \} h d\xi \quad (13)$$

Eq. (13) can be expressed in matrix form and the solution of unknown coefficients is obtained numerically from $\{c\} = [\mathbf{K}]^{-1} \{R\}$ using standard IMSL subroutines and an in-house FORTRAN code. The solution of Eq. (13), at each load step, yields the displacement field from which strains and then stresses were identified.

4. Results and discussions

The material properties of Al-SiC were taken from Shackelford and Alexander (2001), the value of Young's modulus of elasticity for metal (E_m) and ceramic (E_c) were taken as 67 GPa and

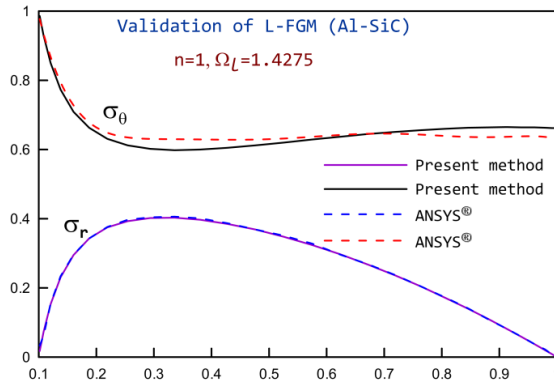


Fig. 4 Validation with finite element analysis

302 GPa respectively. For better understanding, the whole problem was divided into two cases namely-metal rich and ceramic rich. For non-linear distribution of volume fraction variation defined using power-law with grading index (n). Young's modulus and density were calculated using MROM and ROM respectively. Stress plots of different grading parameters were plotted for different aspect ratios to investigate the effect on limit elastic speed due to stresses induced. The location of yielding is plotted along with other stresses, which happens when von Mises and yield stress in a disk becomes equal.

Following are the normalized variables

$$\bar{r} = \frac{r}{b}, \quad \bar{\sigma}_y = \frac{\sigma_y(r)}{\sigma_{y0}}, \quad \bar{\sigma} = \frac{\sigma}{\sigma_{y0}}, \quad \Omega = \omega b \sqrt{\frac{\rho_0}{\sigma_{y0}}},$$

4.1 Validation

For validation of the proposed formulation, a result for grading index ($n = 1$) is compared with result obtained from ANSYS® as shown in Fig. 4. In ANSYS®, uniform thickness disk is modelled with solid 8-noded element (PLANE 183) subject to axisymmetric element behavior under plane stress assumption. Different material property i.e., Young's modulus and density were assigned to each element with the help of macro language. Free-Free boundary condition was given at inner and outer edge and symmetry at the bottom edge. For normalized limit speed, $\Omega_L = 1.4275$, the stresses in an FG rotating disk is calculated. The radial stress and hoop stress of both the methods were compared for Al-SiC FGM's and good agreement between both the methods are seen.

4.2 Stress analysis

Yield stress distributions for different volume compositions were reported, taking yield stress of pure aluminium (σ_{ym}) as 270 MPa. From Eq. (4), it can be seen that yield stress is a function of volume fraction only, as the values of E_c , E_m and parameter R are fixed. So, the qualitative variation of yield stress will be the same as that of volume fraction variation for a particular grading parameter and aspect ratio. Hence, the yield stress variation in Fig. 2, when compared for different grading parameters (n) is found to be the same as that of volume fraction of ceramic as shown in Fig. 1. Fig.

5 shows variation of radial stress, tangential stress, von Mises stress and yield strength of FG disk. The point where the yield stress and von Mises stress coincides is the location of yield and the corresponding speed is the limit elastic speed of the disk. The von Mises stress or effective stress was calculated using Eq. (14). The magnitude of radial stress is increasing as indices (n) increases. Also, the maximum value of radial stress starts shifting towards the center with increasing n . The maximum value of tangential stress increases with the grading indices and so the von Mises stress.

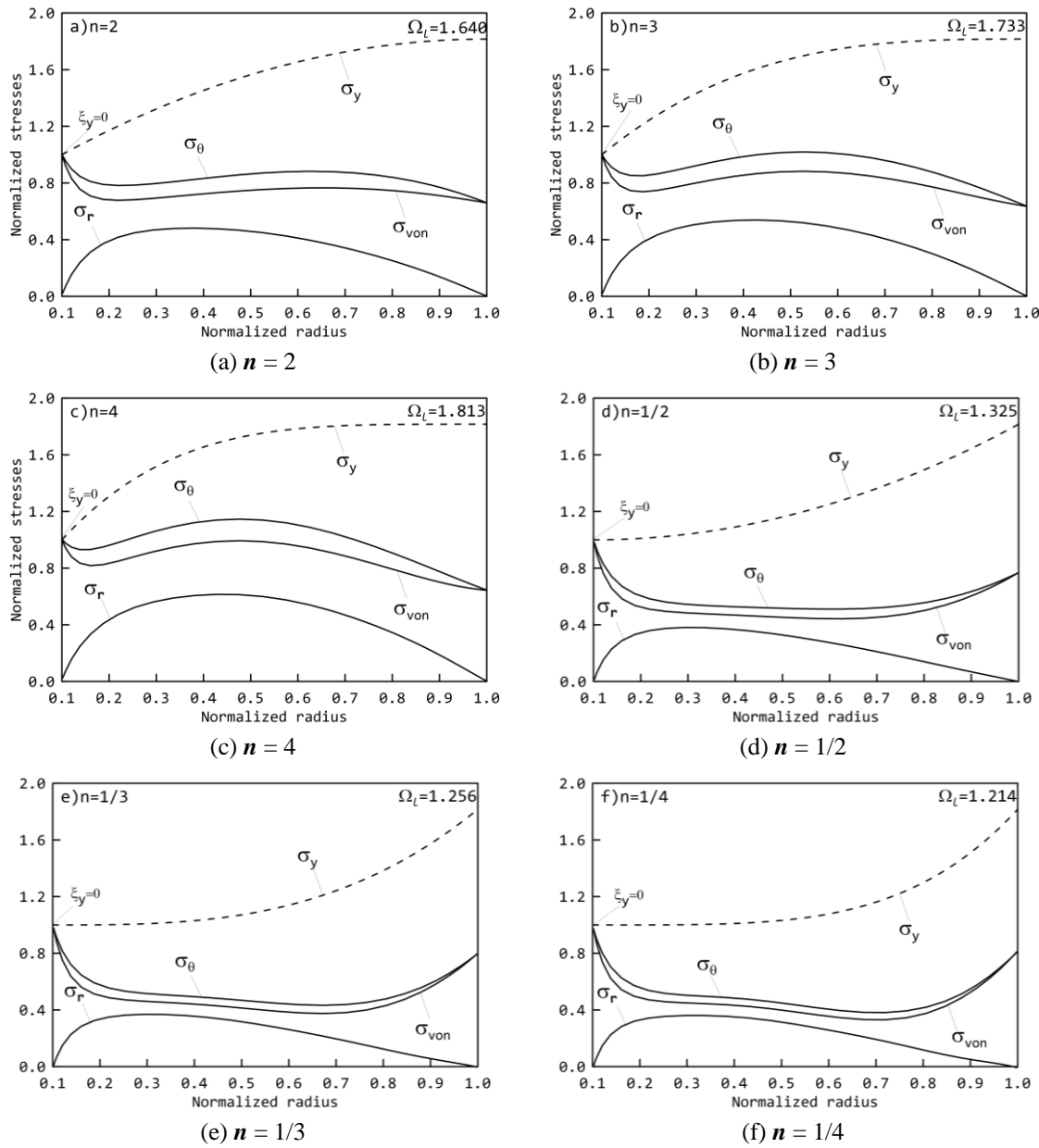


Fig. 5 Stress distribution in uniform thickness disk for $a/b = 0.1$

During rotation, the stresses induced are maximum at the root, for non-linear power-law variation considered the yield stress obtained is minimum at the root, hence, yielding initiates at the root of the disk.

$$\sigma_e^2 = \sigma_r^2 - \sigma_r \sigma_\theta + \sigma_\theta^2 \leq [\sigma_y(r)]^2 \quad (14)$$

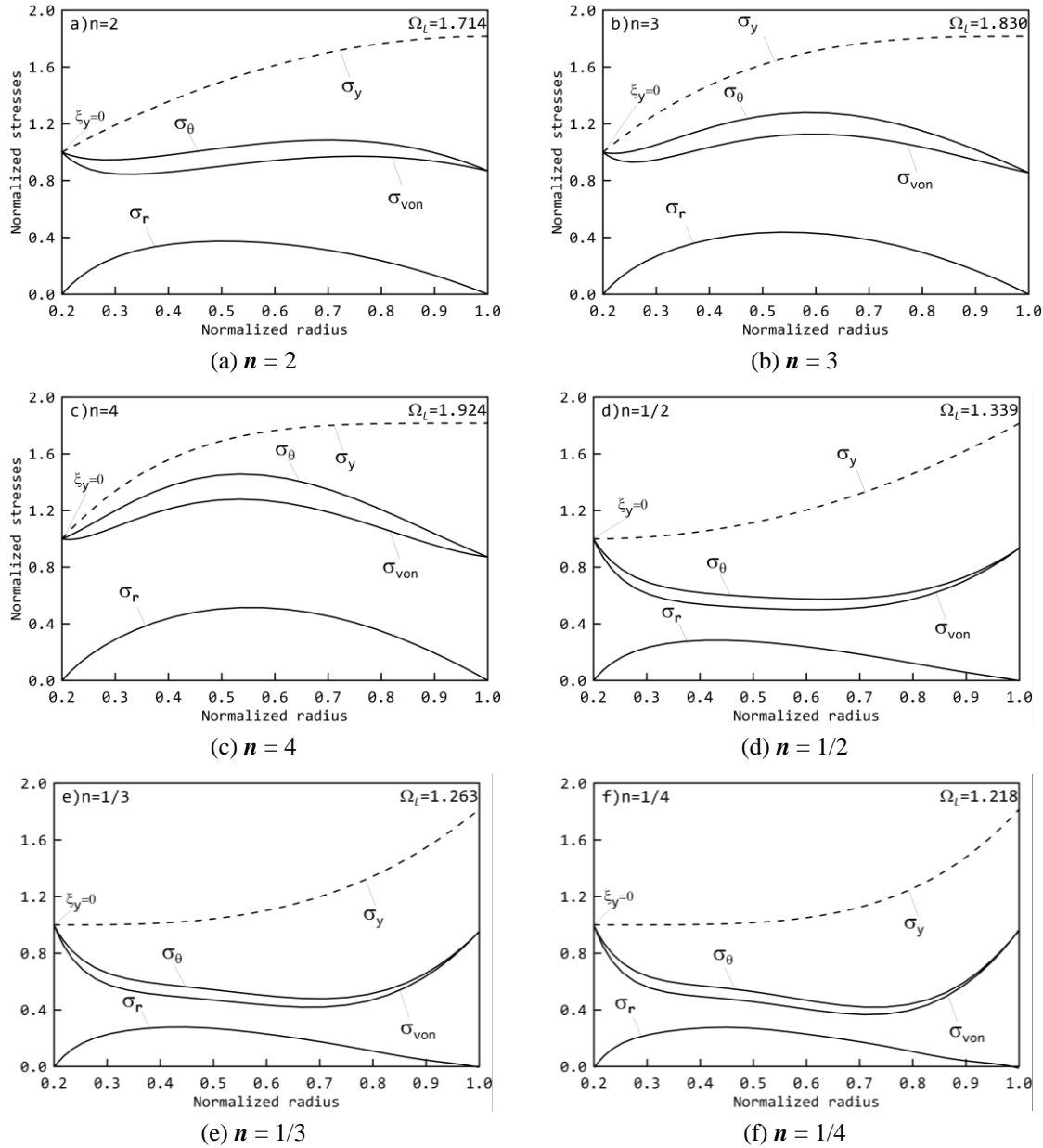


Fig. 6 Stress distribution in uniform thickness disk for $a/b = 0.2$

In Fig. 6, the aspect ratio is 0.2, the behavior of radial stress variation is the same as previous, but the magnitude of radial stress is less for ($a/b = 0.2$). For $n < 1$, the von Mises stress is always maximum at the root but for $n > 1$ its magnitude increases with an increase in n and a stage is reached where the von Mises stress is maximum at the centre, here, it occurs for $n = 3$ and $n = 4$. In Fig. 7, for $a/b = 0.3$, the von Mises stress is maximum at the centre for $n > 1$ and at the root for $n < 1$. The yielding location is at the root in both metal-rich and ceramic rich cases. In Fig. 8, at

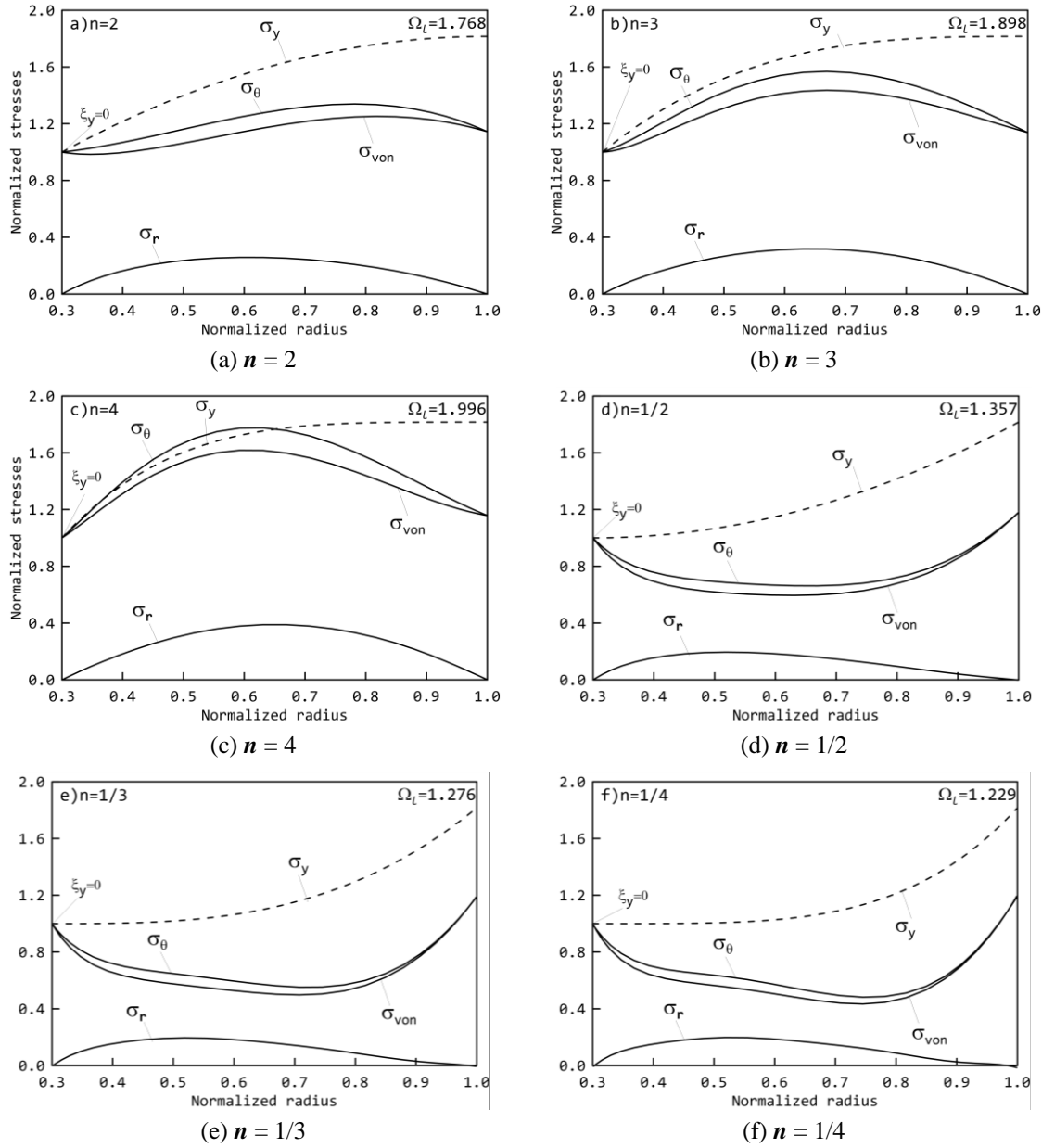
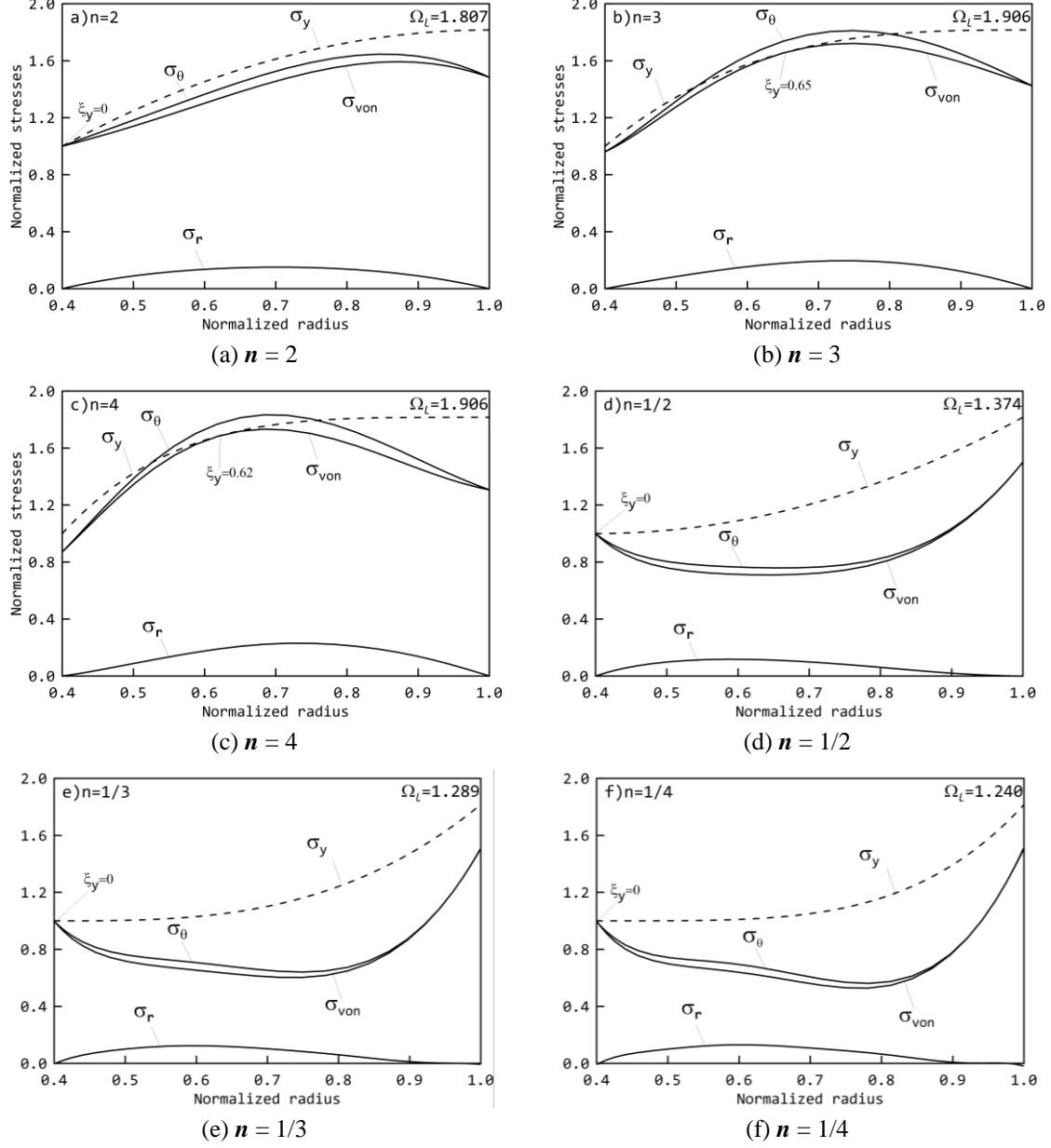


Fig. 7 Stress distribution in uniform thickness disk for $a/b = 0.3$

Fig. 8 Stress distribution in uniform thickness disk for $a/b = 0.4$

$a/b = 0.4$, when $n = 2$, the location of yielding is at the root and as n increases the maximum value of von Mises stress increases at the centre and coincides with the yield near the centre of the disk, resulting in shifting in yielding locations. For $n < 1$, the location of yield initiates at the disk root.

In Fig. 9, for $a/b = 0.5$, unlike all other cases where for $n < 1$ the yielding occurs the tip of the disk were both yield and von Mises is maximum and equal to unity. For $n = 2, 3$ and 4 , the yielding again occurs not at the root but near disk center. In low aspect ratios, yielding always occurs at the

root i.e., till ($a/b = 0.3$) When the aspect ratio is increased further, for $n < 1$, yielding occurs at the disk root for ($a/b = 0.4$) and at the disk tip for ($a/b = 0.5$). In case for ($n = 2$ and $a/b = 0.4$) yielding occurs at the root and when grading index is increased further for $n = 3$ and $n = 4$ the yielding shifts in the left side near the center of the disk. The yield location shifts inside towards the disk root as the grading indices increase as mentioned in Table 1. Table 1 shows the location of yielding for different n and a/b , and the volume composition of ceramic at that location. In case of lower aspect ratio, a gap between von-Mises stress and yield stress is there but the difference becomes minimal as the aspect ratio increases further, this shows that the material grading results in optimized

Table 1 Yield location and its corresponding volume fraction of ceramic

a/b	Yield location and corresponding volume fraction of ceramic ($V_c (%)$)					
	$n = 1/2$	$n = 1/3$	$n = 1/4$	$n = 2$	$n = 3$	$n = 4$
0.1	0.1 (0%)	0.1 (0%)	0.1 (0%)	0.1 (0%)	0.1 (0%)	0.1 (0%)
0.2	0.2 (0%)	0.2 (0%)	0.2 (0%)	0.2 (0%)	0.2 (0%)	0.2 (0%)
0.3	0.3 (0%)	0.3 (0%)	0.3 (0%)	0.3 (0%)	0.3 (0%)	0.3 (0%)
0.4	0.4 (0%)	0.4 (0%)	0.4 (0%)	0.4 (0%)	0.65 (79%)	0.62 (83%)
0.5	1.0 (100%)	1.0 (100%)	1.0 (100%)	0.87 (93%)	0.76 (87%)	0.72 (89%)

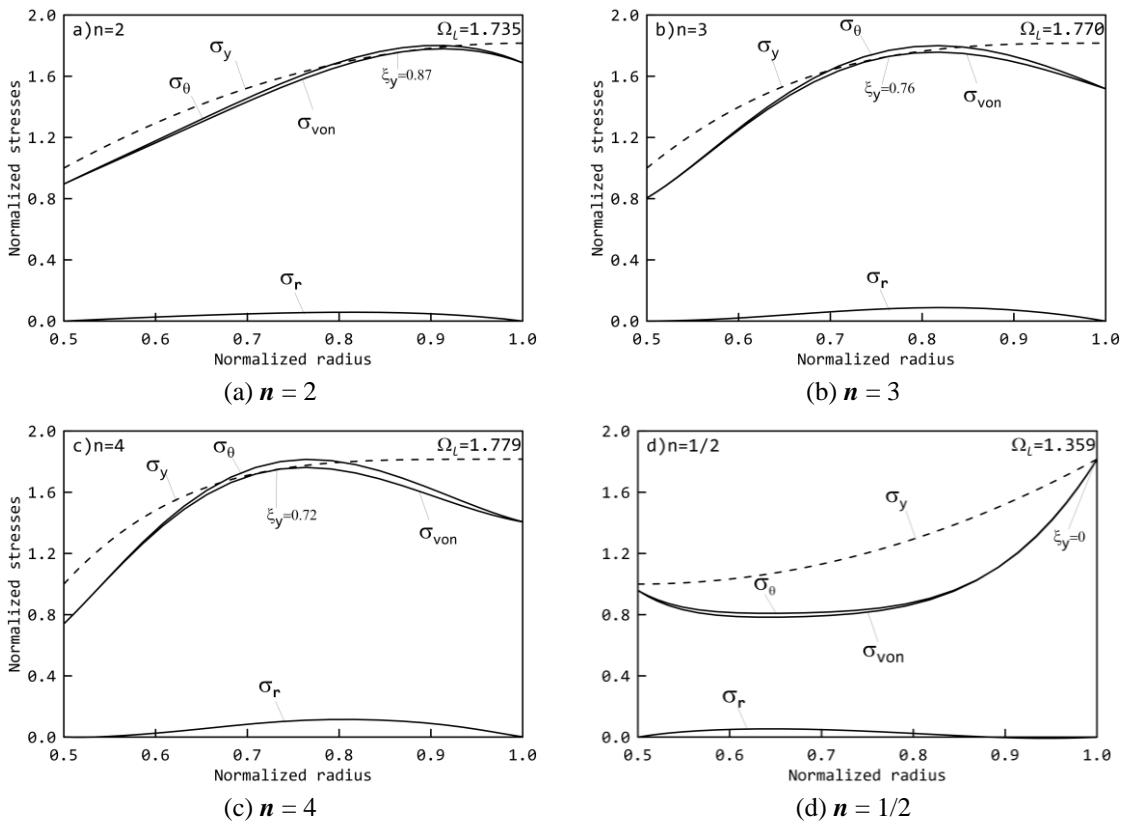


Fig. 9 Stress distribution in uniform thickness disk for aspect ratio = 0.5

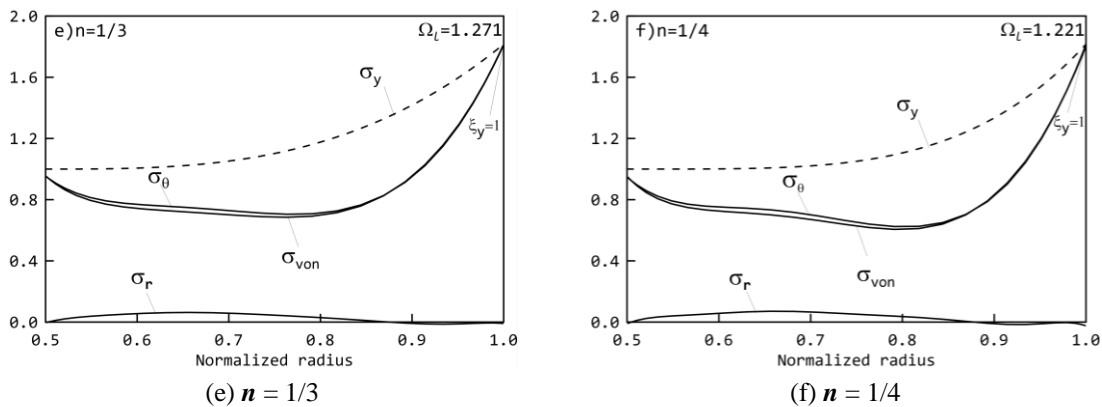


Fig. 9 Continued

Table 2 Normalized limit speed for different grading index and aspect ratios

Aspect ratio	Normalized limit speed					
	$n = 1/2$	$n = 1/3$	$n = 1/4$	$n = 2$	$n = 3$	$n = 4$
0.1	1.325201	1.256726	1.214163	1.640952	1.733587	1.813157
0.2	1.339856	1.263497	1.218355	1.714126	1.830565	1.924558
0.3	1.357959	1.276112	1.229118	1.768422	1.898446	1.996962
0.4	1.374766	1.289271	1.240995	1.807312	1.906067	1.906092
0.5	1.359773	1.271744	1.221809	1.735064	1.770569	1.779385

performance, hence, there is no scope of increasing the limit speed beyond this grading parameters studied.

4.3 Elastic limit analysis

Limit elastic speed analysis was carried out for the same indices and aspect ratio as discussed. The variation in limit speed for different aspect ratios and grading indices is mentioned in Table 2. As the value of n increases limit speed increases for all aspect ratios.

Fig. 10(a), shows limit speed of ceramic-rich compositions, the limit speed first increases with aspect ratios and after reaching a critical value of aspect ratio, here it is 0.4, it starts decreasing. Similar behavior for metal rich can be seen from Fig. 10(b). The qualitative variation of limit speed for different grading indices is the same for metal-rich and ceramic rich. The normalized limit speed for different (n) and different aspect ratios (a/b) is mentioned in Table 2. For analysis purpose the grading index is limited to $n = 4$ and $n = 1/2$, this is to bring both the material contribution in a component, upon increasing the grading index further, the disk will either become pure metal or pure ceramic, to avoid such situations a mixing limitation is imposed by considering a non-linear variation of both the materials. In Table 2, the difference in the limit speed can be seen for varying grading indices (n). As the present analysis is carried out for Al/SiC material, the metal-rich disk (constitutes more of aluminium than silicon carbide) which has a higher limit speed does not incur much difference in manufacturing cost as both the material is available in almost similar price. But in case of nickel as a very costlier metal, such analysis of varying indices as seen here, for $n = 3$ and

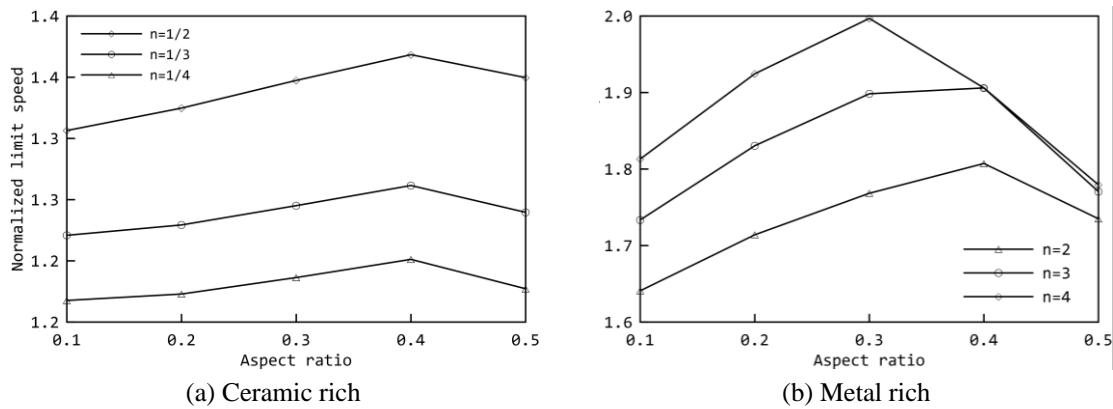


Fig. 10 Limit speed w.r.t aspect ratios for different grading (a) Metal rich; (b) Ceramic rich

$n = 4$ at $a/b = 0.4$ and 0.5 , the limit speed is similar, hence, it can save huge costs if a ceramic can be used as a substitute to nickel (metal) compositions. Also, altering the aspect ratio in a lower index (n), a similar speed as that of higher (n) can be obtained. Similarly, in the case of ceramic rich at $n = 1/2$, limit speed is higher compared to $n = 1/3$ and $1/4$.

5. Conclusions

Limit elastic analysis is performed for a disk with a non-linear variation of metal and ceramic compositions, the following are the conclusion drawn:

- (1) Limit elastic speed of the disk increases when grading indices (n) increases in case of metal-rich, whereas for ceramic rich limit speed is higher for $n = 1/2$, compared to $n = 1/3$ and $n = 1/4$.
- (2) For aspect ratio increase, it increases first for all grading indices till aspect ratio ($a/b \leq 0.4$) in case of ceramic rich and then decreases on further increase in aspect ratios. In the case of metal-rich, limit speed increases up to $a/b = 0.3$ for $n = 4$ and $a/b = 0.4$ for $n = 2$ and 3 .
- (3) The location of yielding is at the root for $n < 1$, till $a/b \leq 0.4$, and at the tip for $a/b = 0.5$. For $n > 1$ the yield location is at the root till $a/b = 0.3$ and near the centre of the disk for further aspect ratio increase. A shift in yielding location is seen for uniform thickness disk in contrast to previous works of literature which states yielding will be at the root for uniform thickness disk.

References

- Abderezzak, R., Rabia, B., Daouadji, T.H., Abbes, B., Belkacem, A. and Abbes, F. (2018), "Elastic analysis of interfacial stresses in prestressed PFGM-RC hybrid beams", *Adv. Mater. Res., Int. J.*, **7**(2), 83-103.
<https://doi.org/10.12989/amr.2018.7.2.83>
- Bayat, M., Saleem, M., Sahari, B.B., Hamouda, A.M.S. and Mahdi, E. (2008), "Analysis of functionally graded rotating disks with variable thickness", *Mech. Res. Commun.*, **35**(5), 283-309.
<https://doi.org/10.1016/j.mechrescom.2008.02.007>

- Bhattacharyya, M., Kapuria, S. and Kumar, A.N. (2007), "On the Stress to Strain Transfer Ratio and Elastic Deflection Behavior for Al/SiC Functionally Graded Material", *Mech. Adv. Mater. Struct.*, **14**(4), 295-302. <https://doi.org/10.1080/15376490600817917>
- Bhowmick, S., Misra, D. and Nath Saha, K. (2008), "Approximate solution of limit angular speed for externally loaded rotating solid disk", *Int. J. Mech. Sci.*, **50**(2), 163-174. <https://doi.org/10.1016/j.ijmecsci.2007.07.004>
- Bhowmick, S., Misra, D. and Saha, K.N. (2009), "A parametric study on the growth of yield front in rotating annular disks", *Int. J. Eng. Sci. Technol.*, **1**(1), 190-204. 7
- Bhowmick, S., Misra, D. and Saha, K. (2010), "Variational formulation based analysis on growth of yield front in high speed rotating solid disks", *Int. J. Eng. Sci. Technol.*, **2**(4), 200-219.
- Çallıoğlu, H., Sayer, M. and Demir, E. (2015), "Elastic–plastic stress analysis of rotating functionally graded discs", *Thin-Wall. Struct.*, **94**, 38-44. <https://doi.org/10.1016/j.tws.2015.03.016>
- Ebrahimi, F. and Jafari, A. (2016), "A higher-order thermomechanical vibration analysis of temperature-dependent FGM beams with porosities", *J. Eng.*, 1-20. <https://doi.org/10.1155/2016/9561504>
- Ebrahimi, F. and Salari, E. (2015), "Thermo-mechanical vibration analysis of nonlocal temperature-dependent FG nanobeams with various boundary conditions", *Compos. Part B: Eng.*, **78**, 272-290. <https://doi.org/10.1016/j.compositesb.2015.03.068>
- Ebrahimi, F. and Salari, E. (2016), "Effect of various thermal loadings on buckling and vibrational characteristics of nonlocal temperature-dependent functionally graded nanobeams", *Mech. Adv. Mater. Struct.*, **23**(12), 1379-1397. <https://doi.org/10.1080/15376494.2015.1091524>
- Ebrahimi, F., Salari, E. and Hosseini, S.A.H. (2015), "Thermomechanical vibration behavior of FG nanobeams subjected to linear and non-linear temperature distributions", *J. Thermal Stress.*, **38**(12), 1360-1386. <https://doi.org/10.1080/01495739.2015.1073980>
- Ebrahimi, F., Salari, E. and Hosseini, S.A.H. (2016), "In-plane thermal loading effects on vibrational characteristics of functionally graded nanobeams", *Meccanica*, **51**(4), 951-977. <https://doi.org/10.1007/s11012-015-0248-3>
- Ebrahimi, F., Mahmoodi, F. and Barati, M.R. (2017), "Thermo-mechanical vibration analysis of functionally graded micro/nanoscale beams with porosities based on modified couple stress theory", *Adv. Mater. Res., Int. J.*, **6**(3), 279-301. <https://doi.org/10.12989/amr.2017.6.3.279>
- Hamed, M.A., Sadoun, A.M. and Eltaher, M.A. (2019), "Effects of porosity models on static behavior of size dependent functionally graded beam", *Struct. Eng. Mech., Int. J.*, **71**(1), 89-98. <https://doi.org/10.12989/sem.2019.71.1.089>
- Jahromi, B.H., Nayeb-Hashemi, H. and Vaziri, A. (2012), "Elasto-plastic stresses in a functionally graded rotating disk", *J. Eng. Mater. Technol.*, **134**(2), 021004. <https://doi.org/10.1115/1.4006023>
- Jha, K., Kumar, R., Verma, K., Chaudhary, B., Tyagi, Y.K. and Singh, S. (2018), "Application of modified TOPSIS technique in deciding optimal combination for bio-degradable composite", *Vacuum*, **157**, 259-267. <https://doi.org/10.1016/j.vacuum.2018.08.063>
- Kordkheili, S.A.H. and Naghdabadi, R. (2007), "Thermoelastic analysis of a functionally graded rotating disk", *Compos. Struct.*, **79**(4), 508-516. <https://doi.org/10.1016/j.compstruct.2006.02.010>
- Madan, R. and Bhowmick, S. (2020), "A review on application of FGM fabricated using solid-state processes", *Adv. Mater. Process. Technol.*, 1-12. <https://doi.org/10.1080/2374068X.2020.1731153>
- Madan, R., Bhowmick, S. and Nath Saha, K. (2018), "Stress and deformation of functionally graded rotating disk based on modified rule of mixture", *Mater. Today: Proceedings*, **5**(9), 17778-17785. <https://doi.org/10.1016/j.matpr.2018.06.102>
- Madan, R., Saha, K. and Bhowmick, S. (2019a), "Limit elastic analysis of rotating annular disks having sigmoid-FGM composition based on MROM", *World J. Eng.*, **16**(6), 806-813. <https://doi.org/10.1108/WJE-05-2019-0155>
- Madan, R., Saha, K. and Bhowmick, S. (2019b), "Limit Elastic Analysis of E-FGM Rotating Disk with Temperature Dependent Mechanical Properties", *Mathe. Model. Eng. Problems*, **6**(4), 634-640. <https://doi.org/10.18280/mmep.060419>
- Madan, R., Bhowmick, S. and Saha, K. (2019c), "Limit angular speed of L-FGM rotating disk for both

- temperature dependent and temperature independent mechanical properties. *Materials Today: Proceedings*, **18**, 2366–2373. <https://doi.org/10.1016/j.matpr.2019.07.080>
- Madan, R., Bhowmick, S. and Saha, K. (2020), “A Study based on Stress-Strain Transfer Ratio Calculation using Halpin-Tsai and MROM Material Model for Limit Elastic Analysis of Metal Matrix FG Rotating disk”, *FME Transact.*, **48**, 204-210. <https://doi.org/10.5937/fmet2001204R>
- Mahamood, R.M. and Akinlabi, E.T. (2017), “Future Research Direction in Functionally Graded Materials and Summary”, In: *Functionally Graded Materials*, (R.M. Mahamood and E.T. Akinlabi), pp. 93-103. https://doi.org/10.1007/978-3-319-53756-6_6
- Mahdavi, E., Ghasemi, A. and Alashti, R.A. (2016), “Elastic–plastic analysis of functionally graded rotating disks with variable thickness and temperature-dependent material properties under mechanical loading and unloading”, *Aerospace Sci. Technol.*, **59**, 57-68. <https://doi.org/10.1016/j.ast.2016.10.011>
- Miyamoto, Y., Kaysser, W.A., Rabin, B.H., Kawasaki, A. and Ford, R.G. (Eds.) (1999), *Functionally Graded Materials*, (Volume 5), Springer US. <https://doi.org/10.1007/978-1-4615-5301-4>
- Mortensen, A. and Suresh, S. (1995), “Functionally graded metals and metal-ceramic composites: Part 1 Processing”, *Int. Mater. Rev.*, **40**(6), 239-265. <https://doi.org/10.1179/imr.1995.40.6.239>
- Nakamura, T., Wang, T. and Sampath, S. (2000), “Determination of properties of graded materials by inverse analysis and instrumented indentation”, *Acta Materialia*, **48**(17), 4293-4306. [https://doi.org/10.1016/S1359-6454\(00\)00217-2](https://doi.org/10.1016/S1359-6454(00)00217-2)
- Nayak, P. and Saha, K. (2016), “Elastic limit angular speed of solid and annular disks under thermomechanical loading”, *Int. J. Eng. Sci. Technol.*, **8**(2), 30. <https://doi.org/10.4314/ijest.v8i2.3>
- Nejad, M.Z., Rastgoo, A. and Hadi, A. (2014), “Exact elasto-plastic analysis of rotating disks made of functionally graded materials”, *Int. J. Eng. Sci.*, **85**, 47-57. <https://doi.org/10.1016/j.ijengsci.2014.07.009>
- Nie, G.J. and Batra, R.C. (2010), “Stress analysis and material tailoring in isotropic linear thermoelastic incompressible functionally graded rotating disks of variable thickness”, *Compos. Struct.*, **92**(3), 720-729. <https://doi.org/10.1016/j.compstruct.2009.08.052>
- Saif, M., Mullick, P. and Imam, A. (2019), “Analysis and structural design of various turbine blades under variable conditions: A review”, *Adv. Mater. Res., Int. J.*, **8**(1), 11-24. <https://doi.org/10.12989/amr.2019.8.1.011>
- Shackelford, J.F. and Alexander, W. (Eds.) (2001), *CRC Materials Science and Engineering Handbook*, (3rd ed.), CRC Press.
- Zheng, Y., Bahaloo, H., Mousanezhad, D., Mahdi, E., Vaziri, A. and Nayeb-Hashemi, H. (2016), “Stress analysis in functionally graded rotating disks with non-uniform thickness and variable angular velocity”, *Int. J. Mech. Sci.*, **119**, 283-293. <https://doi.org/10.1016/j.ijmecsci.2016.10.018>